

Analytical Methods

Accepted Manuscript



This is an *Accepted Manuscript*, which has been through the Royal Society of Chemistry peer review process and has been accepted for publication.

Accepted Manuscripts are published online shortly after acceptance, before technical editing, formatting and proof reading. Using this free service, authors can make their results available to the community, in citable form, before we publish the edited article. We will replace this *Accepted Manuscript* with the edited and formatted *Advance Article* as soon as it is available.

You can find more information about *Accepted Manuscripts* in the [Information for Authors](#).

Please note that technical editing may introduce minor changes to the text and/or graphics, which may alter content. The journal's standard [Terms & Conditions](#) and the [Ethical guidelines](#) still apply. In no event shall the Royal Society of Chemistry be held responsible for any errors or omissions in this *Accepted Manuscript* or any consequences arising from the use of any information it contains.

Phone: +55 19 35213164 / Fax: +55 19 35213023

Fast detection of paracetamol on gold nanoparticles-chitosan substrate by SERS

Abstract

A fast method of detecting pharmaceutical drugs, such as paracetamol, by surface-enhanced Raman spectroscopy (SERS) using gold nanoparticles substrate was studied. Gold nanoparticles were synthesized using chitosan (AuNPs-chitosan) as reductant and capping agent and subsequently deposited on glass slides as a thin film. The SERS performance of AuNPs-chitosan films were evaluated using methylene blue (MB, 10^{-6} mol L⁻¹) as SERS probe molecule. The method is based in drop-drying an analyte solution (paracetamol, 10^{-3} mol L⁻¹) onto substrate surface and subsequently analyzed by Raman spectroscopy. The spectra were obtained in 10 seconds with two accumulations and exhibit an high signal-to-noise ratio. This preliminary study supports AuNPs-chitosan substrate as a SERS sensor, convenient analytical method for paracetamol detection and other pharmaceutical drugs molecules.

Keywords: gold nanoparticles, chitosan, SERS sensor, molecules detection.

Introduction

The occurrence and fate of pharmaceutical compounds in aquatic environment has been recognized as one of the emerging issues in environmental chemistry.^{1,2} Depending on the area many of these compounds are found in concentrations of around $\mu\text{g/kg}$, ng/kg and so on.^{1,2} For example, 4-Hydroxyacetanilide, also named paracetamol and acetaminophen, is one of the most frequently used analgesic and antipyretic drugs.³ As other analgesic drugs, paracetamol rapidly becomes absorbed and distributed after oral administration and it is easily excreted in urine.⁴ The presence of pharmaceuticals from human medical care in aquatic environment may, however, also be caused by others sources such as landfill leachates,⁵ disposal of unused medication via the toilet,⁶ and manufacturing residues.⁷ Several works have shown some evidences that substances of pharmaceutical origin are often not eliminated during the waste water treatment and also not biodegraded in the environment.^{8,9} In this context, fast methods for determination of this kind of compounds can be an efficient strategy to investigate the quality of the water after the waste water treatment. For this purpose, recently, several investigations have shown some methodologies, using SERS/Raman spectroscopy as analytical tool, to detect molecules that are found in samples collected in aquatic environment.¹⁰⁻¹²

Raman spectroscopy is a fast and non-destructive technique and it can be carried out directly on the samples without any extensive sample preparation.^{13,14} However, the low strength of the Raman signal is a limitation to detect molecules in low concentrations, since the Raman line is directly proportional to the concentration of the scattering component of a sample in a laser beam.^{15,16} Moreover, the intensity of Raman scattering (characterized by the Raman cross-section) can vary by many orders of magnitude depending on the molecules under study and the incident laser. It is

important to clarify here that the condition for a molecule to be a "good Raman scattering" is not enough to make it a good SERS probe.^{15,16} Then, a study of the individual Raman spectrum of the target molecule in SERS condition is an important step before proceeding with the application.

The challenge of detecting chemicals in low concentrations has been overcome by using surface enhanced Raman spectroscopy.^{17,18} SERS relies on electronic and chemical interactions among the excitation laser, molecule of interest, and the SERS substrate.¹⁴ The nature of the SERS enhancement of the Raman signal is caused by two contributing mechanisms.^{14,15} First, is the electromagnetic mechanism (long-range), that is a consequence of the interaction of the electric field (from the incident radiation) with the electrons in the metal surface, leading the excitation of surface plasmon. The second mechanism (short-range) is due to charge-transfer from the metal to the molecules adsorbed on the metallic substrate surface. The maximum SERS enhancement, up to 10^{14} -fold the normal Raman signal, typically is observed at specific positions in the substrate surface (hot spots) and only those molecule adsorbed there can gain from it. Substrates that sustain high magnitude of the SERS enhancement have been applied in the detection of biological and chemical species in several kinds of samples with high sensitivity.¹⁶⁻¹⁸

The stabilization of Ag and Au nanoparticles with reductant and capping agents have been reported as a promise strategy to prepare stable and efficient SERS substrates.^{10,11,19-21} Chen *et al.* demonstrated a simple method to detect sulfide in environmental and biological media at the nM level by SERS using silver nanoparticles substrate.¹⁰ Péron *at al.* described a quantitative SERS sensor based on gold nanoparticles for environmental analysis of naphthalene in the range of 1-20 ppm.¹¹ In this work, is reported a simple and fast SERS sensing method for the detection of

pharmaceuticals drugs, such as paracetamol with high sensitivity. For this purpose, gold nanoparticles was synthesized using chitosan as reductant and capping agent, and subsequently deposited as a thin film on glass slides. The SERS properties of the material were probed using methylene blue as Raman probe molecule. Thus, to evaluate the possibility of employing the AuNPs-chitosan substrate in future applications, as a platform in the detection and analysis of pharmaceutical drugs, it was tested to detect paracetamol in a simple and fast method.

Experimental

Chitosan powder sample (high molecular weight, 78% deacetylated) was acquired for free from C.E. Roeper, Hamburg - Germany. Tetrachloroauric(III) acid, 3-mercaptopropyl-trimethoxysilane (MPTMS), methylene blue and 4-hydroxyacetanilide (paracetamol) were purchased from Sigma-Aldrich. All chemicals were used without further purification. All glassware were cleaned with piranha solution (4:1 sulphuric acid:hydrogen peroxide) before using and then rinsed thoroughly with deionized water.

AuNPs were prepared following the procedure reported elsewhere with some modifications.²² Briefly, a solution of chitosan 1 mg mL⁻¹ was prepared by dissolving the polymer in acid acetic solution (pH = 2.5). Due to the low solubility of chitosan, the mixture was kept under stirring for 8 h to obtain a clear solution. A mixture of 6 mL solution of 10⁻³ mol L⁻¹ tetrachloroauric(III) acid and 36 mL solution of 1 mg mL⁻¹ chitosan was prepared. The AuNPs-chitosan synthesis was carried out under stirring at 100 °C for 10 min, resulting in a red color solution.

Microscope regular glass slides were cut in 1.2 cm² pieces, cleaned, and their surfaces were modified following the procedure reported elsewhere, but in the present work using MPTMS.²³ The AuNPs-chitosan films were prepared by dropping 100 µL of

AuNPs solution onto thiol groups modified glass pieces. To solvent evaporation the pieces were placed into an oven at 50 °C for 15 min. To complete the films preparation this procedure was repeated more two times, drop-drying a total volume of 300 μL for each AuNPs-chitosan film prepared. Before the second and third AuNPs-chitosan deposition the films were washed with deionized water to displace any residual material of the synthesis and dried with N_2 flow.

UV-visible absorption spectra of the AuNPs-chitosan solution and of the AuNPs-chitosan films were collected on an Agilent Cary probe 50 UV-vis spectrometer. High resolution transmission electron microscopy (HRTEM) images were obtained using a JEOL JEM-3010 microscope (300 kV, 1.7 Å point resolution). The sample was prepared by drop-drying the AuNPs-chitosan solution on a holey carbon coated Cu grid. SERS spectra were acquired using a confocal Jobin-Yvon T64000 Raman spectrometer system, equipped with a liquid- N_2 -cooled CCD. The excitation source was a laser at 633 nm. The laser power at the sample surface was about 7.2 mW. The laser was focused with a 100x focal-lens objective to a spot of about 1 μm . For all measurements, the laser exposure time was 10 s with two accumulation. An aliquot of 50 μL of MB (10^{-6} mol L^{-1}) aqueous solution was dropped onto the 1.2 cm^2 AuNPs-chitosan film surface. The film was dried in air atmosphere. After that, the sample was ready to be analyzed. The same procedure was used to detect paracetamol (10^{-3} mol L^{-1}).

135

136 Results and discussion

Figure 1(a) shows the UV-vis absorption spectrum of the AuNPs-chitosan solution with surface plasmon band at 525 nm. This is the standard optical signature for the formation of AuNPs spheres in solution. A representative AuNPs-chitosan film

140 shows the surface plasmon band at 537 nm, indicating a red shift of 12 nm in the
141 absorption maximum (Fig. 1(b)). This red shift is caused due to increase the refractive
142 index of the media surrounding metallic nanoparticles.^{24,25} The UV-vis spectral profile
143 of the chitosan solution (Fig. 1(c)) does not shows any absorption band at UV-vis range.
144 As observed in the HRTEM image in Fig. 2(a) the AuNPs are immersed into the
145 chitosan structure forming a composite. Measuring the AuNPs diameter, in different
146 HRTEM images, is obtained an average size distribution of 5.2 nm (Fig. 2(b)). The
147 narrow size distribution (1.5 - 12.5 nm) indicates that chitosan plays an important role
148 of controlling the AuNPs size as well as provides a high density of gold nanoparticles
149 on its structure. That condition is related with the short distance among the AuNPs
150 immersed into the chitosan structure, being an appropriate condition to plasmon
151 coupling, which promoted Raman signal enhancement.

152
153 **Insert Figure 1**

154
155 **Insert Figure 2**

156
157
158 As shown in the literature, stable gold nanoparticles can be easily synthesized
159 with excellent size control using chitosan as reductant and capping agent.^{26,27} Its dual
160 role is a great advantage, once it is not necessary add other compound to promote the
161 reaction. Despite the widespread use of chitosan in the gold nanoparticles synthesis, the
162 reaction mechanism has not been explained. In the present work, the gold nanoparticles
163 synthesis using chitosan was conducted in acetic acid solution. In that condition, the
164 chitosan is soluble and the amine groups can be protonated ($-NH_3^+$), consequently, this

1
2
3 165 biopolymer reach a positive residual charge. Then, these groups can to attract the AuCl_4^-
4
5 166 ions from the solution, suggesting that they are the sites where the reduction step takes
6
7 167 place to size-controllable AuNPs. Finally, the chitosan chains, loaded of AuNPs, self-
8
9 168 assemble into larger structures as shown in Fig. 2(a). The overall reaction could be
10
11 169 represented as illustrated in Fig. 3 according to our results and to some related
12
13 170 researches.^{26,27}
14
15
16
17
18
19
20
21
22
23
24
25
26
27
28
29
30
31
32
33
34
35
36
37
38
39
40
41
42
43
44
45
46
47
48
49
50
51
52
53
54
55
56
57
58
59
60

171
172
173 **Insert Figure 3**
174
175

176 To evaluate the SERS efficacy of the AuNPs-chitosan film, Raman
177 measurements were conducted employing MB as the model molecule. As shown in Fig
178 4(a), it is clear that the characteristic Raman bands of MB are very weak to be observed
179 and the spectrum was multiplied twenty times. The bands of MB at 1622 and 446 cm^{-1} ,
180 which have been assigned to C-C stretching and C-N-C skeletal bending, respectively,
181 are the most intense bands in the SERS spectrum (Fig. 4(b)). This result indicates that
182 the MB molecules were adsorbed on the AuNPs-chitosan substrate.^{28,29} The bands at
183 236 and 306 cm^{-1} , that were not observed in the powder MB spectrum can be ascribed
184 to Au-N and Au-S stretching of the Au-MB complex, respectively.^{29,30} The bands at
185 360, 670, 1031, and 1230 cm^{-1} are observed only in the MB SERS spectrum (Fig. 4(b)).
186 At the same time, the intensities of the bands at 478 and 888 cm^{-1} are very prominent in
187 the SERS condition, that is a strong evidence of this enhancement effect.
188
189

190

191

Insert Figure 4

192

193

194 To check the repeatability of the SERS spectra, measurements were made in five
195 different points, randomly chosen, in the same AuNPs-chitosan film. The MB Raman
196 signature is observed in all collected SERS spectra (Fig. 5). The difference was only
197 between the relative intensities of the spectra collected from point-to-point, while the
198 spectral position and the full width of Raman bands show no noticeable difference (Fig.
199 5). The band at 1622 cm⁻¹ exhibit the highest intensity, indicating that this band can be
200 used as MB reference in future analyses.

201

202

203

Insert Figure 5

204

205

206 The Raman signal scattered from the chitosan is very weak and it does not
207 interfere in SERS spectra of MB model molecule (Fig. 5). This is an interesting result,
208 indicating that this kind of substrate can be employed to detect molecules without any
209 interference from the substrate background. As a demonstration of a practical
210 application of the above AuNPs-chitosan substrate, it was tested as SERS sensor to
211 detect paracetamol. Fig. 6 shows the measured SERS spectra for paracetamol powder
212 and for paracetamol after drop-drying 50 µL of 10⁻³ mol L⁻¹ solution on the AuNPs-
213 chitosan substrate. The SERS spectra differ mainly in intensity and positions when
214 comparing with the Raman spectrum of the paracetamol powder. Also, the SERS

spectra differ each other (Fig. 6 (b) and (c)). This can be explained based on paracetamol chemical structure,³¹ that can undergo deprotonation and achieve a stable equilibrium in water (inset Fig. 6). Both structures, paracetamol and its conjugated base (oxyanion), can interact with the AuNPs-chitosan substrate in different ways due to their different charges. In that situation molecules can be differently orientated on the sensor surface, resulting in different intensities and positions of some Raman bands as observed in Fig. 6.

Insert Figure 6

The band at 1168 cm^{-1} for $\sigma^{\text{ip}}(\text{HCC})$, ip: in-plane) and for $\square(\text{CC})$ is shifted to 1145 and 1154 cm^{-1} and also is observed in the SERS spectrum in Fig. 6(C), indicating that there are molecules attached on the AuNPs-chitosan substrate surface with different orientations.^{32,33} The band at 1237 cm^{-1} for $\square(\text{CC})$ and $\sigma^{\text{ip}}(\text{HOC})$ is observed in both SERS spectra, appearing as shoulder in the spectrum in Fig. 6(C). The band at 1258 cm^{-1} for $\square(\text{C-O})$, $\sigma^{\text{ip}}(\text{HCC})$ and $\square(\text{CC})$ appear only in the spectrum in Fig. 6(C) as the highest one, indicating that the SERS effect is operating on the system. The band at 1325 cm^{-1} , attributed to Amide III band (C-N stretch/C-N-phenyl stretch/C-N-H band), is split and becomes more intense in Fig. 6(C). The band at 1371 cm^{-1} for $\sigma^{\text{s}}(\text{CH}_3, \text{s: symmetric})$ appear in different positions in the SERS spectra; unlike the band at 1445 cm^{-1} for $\sigma^{\text{as}}(\text{CH}_3, \text{as: asymmetric})$ is observed in the same position in the SERS spectra, but it is much more intense in Fig. 6(C). The band at 1565 cm^{-1} for $\sigma^{\text{ip}}(\text{HNC})$ and $\square(\text{CC})$ is observed only in Fig. 6(b), while the band at 1585 cm^{-1} for $\square(\text{CC})$ and

240 $\sigma^{\text{ip}}(\text{HNC})$ is observed only in Fig. 6(C).³³ The band at 907 cm^{-1} observed only in Fig.
241 6(b) could not be assigned, since any band was observed in this position in the
242 paracetamol powder Raman spectrum. These changes observed in the SERS spectra
243 bands are correlated with orientation differences in the paracetamol molecules adsorbed
244 on the AuNPs-chitosan SERS sensor. The high intensity observed for some bands, in
245 the SERS condition, indicates that the substrate is a promise sensitive sensor to detect
246 paracetamol even in concentrations below $10^{-3} \text{ mol L}^{-1}$. This kind of SERS sensor has
247 potential applications in the analytical field and the straightforward procedure used has
248 several advantages as a fast and efficient method.

249

250 Conclusions

251 AuNPs were synthesized in a simple and convenient method using chitosan as
252 reductant and capping agent. The AuNPs-chitosan composite is easily deposited on
253 glass slide forming a film which exhibited an excellent performance as SERS substrate.
254 AuNPs-chitosan film showed sensitivity to detect MB in low concentration by SERS.
255 Such AuNPs-chitosan film was employed as a SERS sensor to detect and identify
256 paracetamol by drop-drying 50 μL onto the substrate surface. This methodology is
257 simple, fast and cost-effective. Also, the originality and advantage of this SERS-active
258 substrate reside in the fact that the chitosan Raman signal does not interfere on the
259 Raman spectra of the analytes. In the near future, AuNPs-chitosan can be employed as
260 a sensor of other pharmaceutical drugs using the same methodology, even in low
261 concentrations.

262

263

264

Acknowledgments

EBS thanks FAPESP for a post-doc fellowship. The authors would like to thank the FAPESP, CAPES and CNPq for financial supports. Contributions from Multiuser Laboratory of Advanced Optical Spectroscopy (LMEOA/IQ/UNICAMP) for the Raman facilities and Brazilian Nanotechnology National Laboratory (LNNano, Campinas-SP, Brazil) for HRTEM facilities is also grateful. This is a contribution of the National Institute of Science and Technology in Complex Functional Materials (CNPq-MCT/FAPESP).

References

- 1 B. Halling-Sorensen, N. Nielsen, P. F. Lansky, F. Ingersley, L. Hansen, H. C. Lutzhof, S. E. Jorgensen, *Chemosphere*, 1998, 36, 357.
- 2 C. G. Daughton, T. A. Ternes, *Environ. Health Perspect.*, 1999, 107, 907.
- 3 K. Klimova, J. Leitner, *Thermochimica Acta*, 2012, 550, 59.
- 4 J. Parojcic, K. Karljikovic-Rajic, Z. Duric, M. Jovanovic, S. Ibric, *Biopharm. Drug Dispos.*, 2003, 24, 309.
- 5 J. V. Holm, K. Rugge, P. L. Bjerg, T. H. Christensen, *Environ. Sci. Technol.*, 1995, 29, 1415.
- 6 T. A. Ternes, *Water Res.*, 1998, 32, 3245.
- 7 K. Reddersen, T. Heberer, U. Dunnbier, *Chemosphere*, 2002, 49, 539.
- 8 C. Zwiener, T. Glauner, F. H. Frimmel, *High Res. Chromatogr.*, 2000, 23, 474.
- 9 H. R. Buser, T. Poiger, M. D. Muller, *Environ. Sci. Technol.*, 1999, 33, 2529.
- 10 L-X. Xen, Da-W. Li, L-L. Qu, Y-T. Li, Y-T. Long, *Anal. Methods*, 2013, 5, 6579.

289 11 O. Peron, E. Rinnert, T. Toury, M. L. Chapelle, C. Compere, *Analyst*, 2011, 136,
290 1018.

291 12 R. A. Alvarez-Puebla, L. M. Liz-Marzan, *Angew. Chem. Int. Ed.*, 2012, 51,
292 11214.

293 13 M. Fleischmann, P. J. Hendra, A. J. McQuillan, *Chem. Phys. Lett.*, 1974, 26, 63.

294 14 E. C. Le Ru, P. G. Etchegoin, *Principles of Surface-Enhanced Raman*
295 *Spectroscopy*. Amsterdam: Elsevier; 2009.

296 15 R. Aroca, *Surface-enhanced Vibrational Spectroscopy*. Southern Gate: John
297 Wiley & Sons; 2006.

298 16 Y. Zhang, S. Liu, L. Wang, X. Qin, J. Tian, W. Lu, G. Chang, X. Sun, *RSC*
299 *Advances*, 2012, 2, 538.

300 17 G. Moula, R. F. Aroca, *AnaL. Chem.*, 2011, 83, 284.

301 18 W. W. Yu, I. M. White, *Analyst*, 2012, 137, 1168.

302 19 W. L. Zhai, D. W. Li, L. L. Qu, J. S. Fossey, Y. T. Long, *Nanoscale*, 2012, 4,
303 37.

304 20 M. Alsawafta, S. Badilescu, M. Packirisamy, V. V. Truong, *Reac. Kinet. Mech.*
305 *Cat.*, 2011, 104, 437.

306 21 K. Esumi, N. Takei, T. Yoshimura, *Colloids Surf. B*, 2003, 32, 117.

307 22 M. Potara, D. Maniu, S. Astilean, *Nanotechnology*, 2009, 20, 315602.

308 23 E. B. Santos, F. A. Sigoli, I. O. Mazali, *Vib. Spectrosc.*, 2013, 68, 246.

309 24 Y. Q. Wang, W. S. Liang, C. Y. Geng, *Nanoscale Res. Lett.*, 2009, 4, 684.

310 25 E. F. S. Vieira, A. R. Cestari, E. B. Santos, F. S. Dias, *J. Colloid Interf. Sci.*,
311 2005, 289, 42.

312 26 Y-C. Cheng, C-C. Yu, T-Y. Lo, Y-C. Liu, *Mater. Res. Bull.*, 2012, 47, 1107.

313 27 T. T. Nhung, Y. Bu, S-W. Lee, *J. Cryst. Growth*, 2013, 373, 132.

- 1
2
3 314 28 G. N. Xiao, S. Q. Man, *Chem. Phys. Lett.*, 2007, 447, 305.
4
5 315 29 C. M. Ruan, W. Wang, B. H. Gu, *J. Raman Spectrosc.*, 2007, 38, 568.
6
7 316 30 Y. Peng, Z. Niu, W. Huang, S. Chen, Z. Li, *J. Phys. Chem. B*, 2005, 109, 10880.
8
9 317 31 M. A. Elbagerma, G. Azimi, H. G. M. Edwards, A. I. Alajtal, I. J. Scowen,
10
11 318 *Spectrochim Acta Mol. Biomol. Spectros.*, 2010, 75, 1403.
12
13 319 32 B. Chazallon, Y. Celik, C. Focsa, Y. Guinet, *Vib. Spectrosc.*, 2006, 42, 206.
14
15 320 33 J. B. Nanubolu, J. C. Burley, *Mol. Pharmaceutics*, 2012, 9, 1544.
16
17
18 321
19
20
21
22
23
24
25
26
27
28
29
30
31
32
33
34
35
36
37
38
39
40
41
42
43
44
45
46
47
48
49
50
51
52
53
54
55
56
57
58
59
60

322 **FIGURE CAPTIONS**

323

324 **Figure 1.** UV-visible absorption spectra of (a) AuNPs-chitosan solution, (b) a
325 representative film prepared with AuNPs-chitosan, and (c) chitosan solution.

326

327 **Figure 2.** (a) HRTEM image showing the AuNPs into the chitosan structure and (b)
328 Histogram of the AuNPs average size distribution into the chistosan structure.

329

330 **Figure 3.** Simplified schematic representation of the formation of AuNPs-chitosan
331 composite.

332

333 **Figure 4.** (a) Raman spectrum of solid methylene blue powder and (b) SERS spectrum
334 of 10^{-6} mol L⁻¹ methylene blue dropped onto a AuNPs-chitosan film.

335

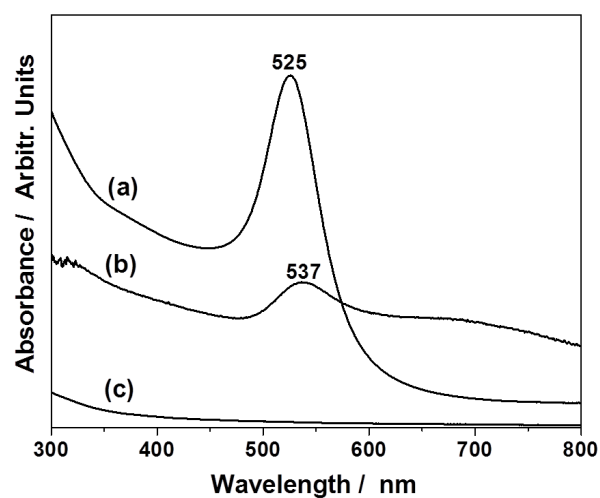
336 **Figure 5.** SERS spectrum of the AuNPs-chitosan substrate and SERS spectra of 10^{-6}
337 mol L⁻¹ methylene blue onto a AuNPs-chitosan film recorded in five different points.

338

339 **Figure 6.** (a) Raman spectrum of paracetamol powder, (b) and (c) SERS spectra of 10^{-3}
340 mol L⁻¹ paracetamol recorded onto a AuNPs-chitosan film. Inset shows the
341 deprotonation equilibrium of paracetamol and its conugated base in water.

342 **Figure 1**

343

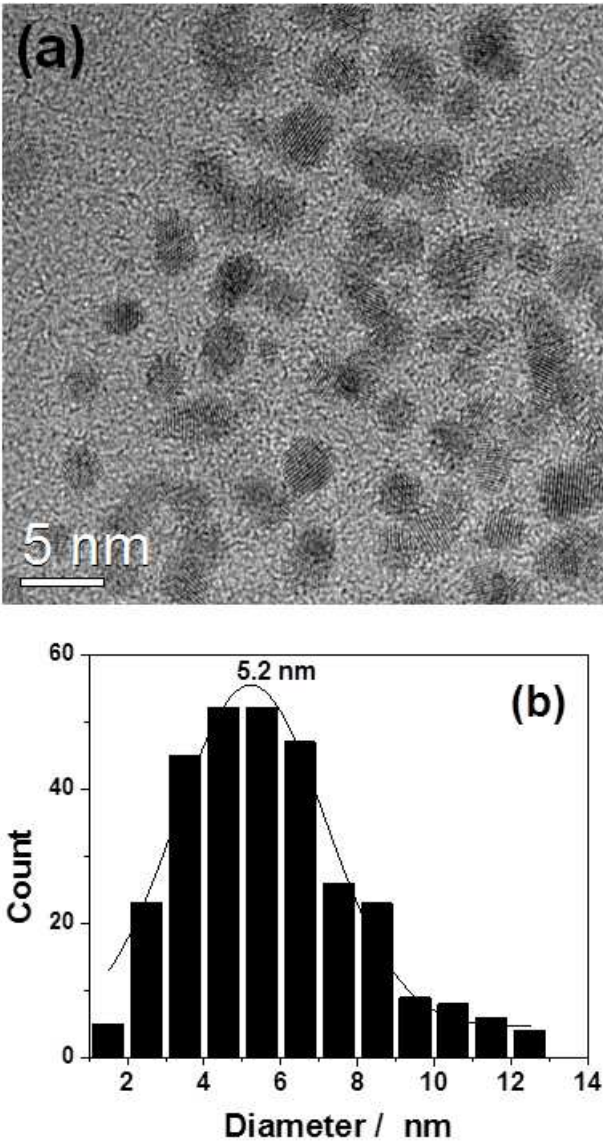


344

345

346 **Figure 2**

347

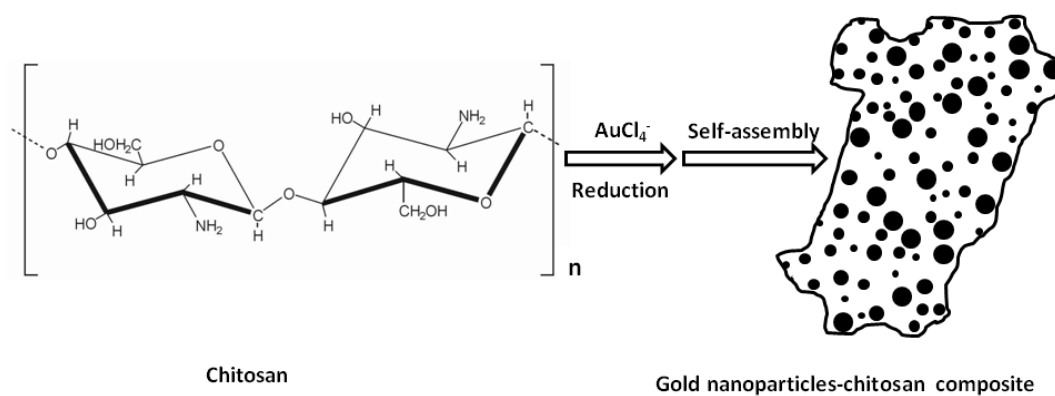


348

349

350 **Figure 3**

351

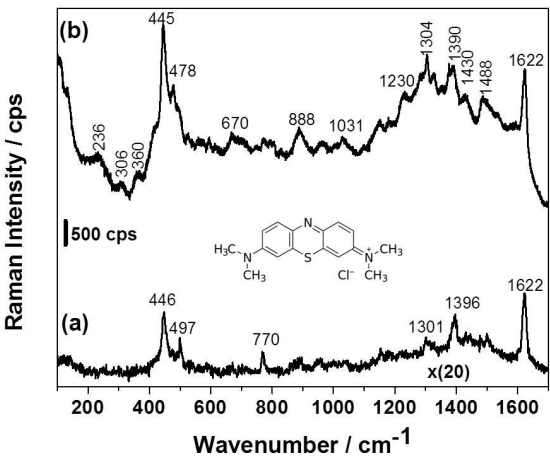


352

353

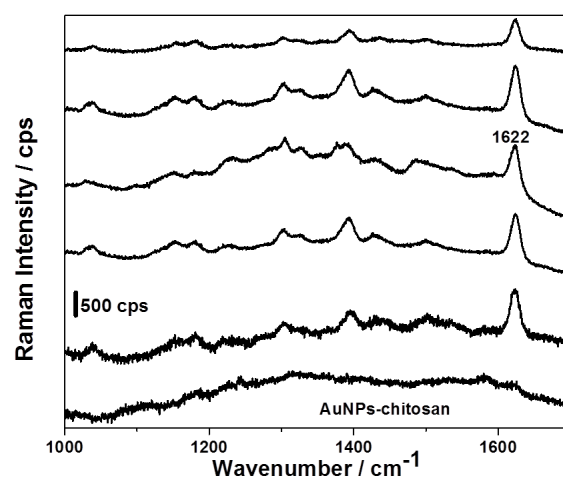
354 **Figure 4**

355



356

357

358 **Figure 5**

359

360

Figure 6.

